

RESEARCH ARTICLE

PI Parameters Tuning for Frequency Tracking Control of Wireless Power Transfer System Based on Improved Whale Optimization Algorithm

XIONG YANG¹ AND JIAMIN GUAN^{1,2}¹Distribution Network Technology Department, State Grid Jiangsu Electric Power Company Ltd., Research Institute (JSEPRI), Nanjing 211103, China²School of Mechanical Engineering, Nanjing Institute of Technology, Nanjing 211167, China

Corresponding author: Jiamin Guan (guanjiamin1127@163.com)


This work was supported in part by the Science and Technology Project of State Grid Jiangsu Electric Power Company Ltd. under Grant J2021016.

ABSTRACT For the efficiency optimization problem of wireless power transfer system, the most important thing is that the frequency tracking control is needed to make the system work in a resonant state. The parameters of the frequency tracking controller directly determine the control performance. In this paper, we consider using an improved whale optimization algorithm to complete the PI parameter tuning of the frequency tracking controller as a way to save personnel's effort and time on the controller design. This improved whale optimization algorithm mainly has the following improvements: firstly, it uses Kent chaotic mapping to initialize the whale population, which improves the variegation of the initial solution; secondly, it introduces adaptive weight coefficients and nonlinearly improves the convergence factor, which achieves a balance between the algorithm's global and local searching ability; finally, it introduces sine-cosine algorithmic strategy and Cauchy reverse learning strategy, which avoids the problem that the algorithm is easy to mature prematurely. The superiority of the improved algorithm is verified through the testing of eight benchmark functions and the Wilcoxon rank sum test method. Finally, the algorithm is applied to the PI parameter optimization of frequency tracking control, and the phase difference curves under the control of different PI parameters are compared by simulation. The results show that the improved algorithm proposed in this paper has a better performance for the PI parameter tuning of frequency tracking control in wireless power transfer system, which can effectively help reduce the investment of human resources.

INDEX TERMS Wireless power transfer, frequency tracking control, PI control, whale optimization algorithm.

I. INTRODUCTION

At present, the magnetically coupled resonance wireless power transfer (MCR-WPT) system has been widely used in electric vehicle wireless charging, health monitoring, embedded devices and other fields due to the advantages of long transmission distance and high transmission efficiency, and has become a research hotspot in the field of wireless charging [1]. However, factors such as ambient temperature, operating conditions, coil size and surface effects may cause variations in the electrical parameters of the system.

The associate editor coordinating the review of this manuscript and approving it for publication was Paolo Crippa .

These variations may result in changes in the actual operating resonant frequency, causing a rapid drop in transmission efficiency. Therefore, keeping the MCR-WPT system operating at resonant frequency is one of the key techniques to improve transmission efficiency [2], [3].

To ensure that the MCR-WPT system operates in a resonant state, the frequency tracking control method is widely used in WPT systems due to its easy implementation and fast response. The frequency tracking control determines the resonant state by detecting the phase difference between the voltage and current at the transmitter. If the MCR-WPT system is detuned, there will be a phase difference between voltage and current. The control system will generate a drive

signal based on the feedback signal of the phase difference and adjust the frequency of the inverter output voltage so that the phase difference will be zero to keep the system in resonance [4]. In order to improve the effect of frequency tracking control, many scholars have introduced the theory of fuzzy rules. By designing fuzzy rules, the frequency tracking control system based on fuzzy PI control has been realized [5], [6], [7]. However, this does not mean that the traditional PID controller is not as effective as it should be. On the contrary, PI controllers are widely used in engineering fields due to their simple structure and easier implementation. As long as the design of reasonable control parameters, the control performance can still meet the needs of actual working conditions.

In recent years, population intelligence algorithms have been gradually applied to various fields, including the optimal tuning of controller parameters. For example, in the field of vehicle cruise control, [8] improved the performance of the reptile search algorithm via the integration of Lévy flight concept and applies it to the parameter tuning of the PID control of the vehicle cruise control system. Reference [9] developed a novel AOA-NM meta-heuristic algorithm and combined it with a PID controller based on Bode's ideal transfer function to achieve optimal performance of the automobile cruise system. In addition, distinguishing from integer-order PID controllers, fractional-order PID (FOPID) is able to more accurately characterize the dynamics of the system by introducing fractional-order differentiation and integration, thus providing better control performance [10]. And population intelligence algorithms for parameter tuning of FOPID controllers have also received attention from many scholars. For example, [11] proposed a novel improved slime mold algorithm to tune the parameters of the FOPID controller and the PIDD² controller, which is applied to speed control of the DC motor and terminal voltage level control of the automatic voltage regulator. Reference [12] used a genetic algorithm and constructed a cost function with respect to the tracking error and control effort to optimize a FOPID controller for a two coupled tanks system. Further, [13] designed a control structure combining fuzzy control and FOPID control for a Buck converter and used an antlion optimization algorithm to adjust the gain of the fuzzy-FOPID.

The application of intelligent optimization algorithms in controller parameter tuning has become increasingly widespread. This is mainly due to the fact that these algorithms are able to efficiently find global optimal or near-optimal solutions in complex, nonlinear and multi-dimensional parameter spaces by simulating evolutionary, population behavior or physical processes in nature, which can significantly improve the performance of the controllers and reduce the time and cost of manual debugging. Therefore, for the WPT frequency tracking control system, intelligent algorithms can also be used to optimize the controller parameters. In this paper, the whale optimization algorithm is chosen to achieve the tuning of the frequency tracking

controller parameters. Whale Optimization Algorithm (WOA) is a bionic intelligence algorithm proposed by MIR-JALILI in 2016 [14], which is simple to operate, requires fewer parameters to be adjusted, and has been commonly used within various engineering fields. However, the whale algorithm is still difficult to avoid the shortcomings of easy to fall into the local optimum, slow convergence of the algorithm and insufficient convergence accuracy. For these problems, scholars have made many improvement measures.

Reference [15] proposed a hybrid algorithm of WOA and PSO, which combines the search ability of WOA and the fast convergence property of PSO. However, in the early stage of the algorithm, WOA and PSO operate independently, and the algorithm does not achieve the full sense of integration. Moreover, in some cases, the characteristics of WOA and PSO may not be fully complementary, resulting in the performance of the hybrid algorithm is even worse than that of one algorithm alone. Reference [16] proposed an improved whale optimization algorithm, which improves the diversity of the initial population by combining logistic chaos mapping and skew tent mapping, and enhances the global search ability by introducing the cross operator and Gaussian variational operators. However, the introduction of more operators and mapping methods leads to over-complexity of the algorithm, which may lead to the generation of overfitting phenomena and affect the generalization ability of the algorithm. Reference [17] enhanced the global search capability of WOA by introducing an inertia weight factor and controlling the value using reinforcement learning techniques and introduced a variable neighborhood search algorithm to improve the local optimization capability. However, the introduction of reinforcement learning techniques requires an appropriate dataset or training process to train the model, which may require additional data collection and processing efforts. Reference [18] optimized the initial population distribution of the algorithm; introduced segmented control parameters and adaptive weights to improve the convergence speed of the algorithm; added an adaptive learning factor to control the variability of each individual's learning ability to improve the algorithm's global searching ability; and introduced a Cauchy perturbation on the optimal individual, which avoids the problem that the algorithm is easy to fall into the local optimum. However, the above strategies emphasize global search, which may lead to premature convergence of the algorithm to a non-global optimal solution. In some cases, the balance between local and global search may be more important. Reference [19] introduced chaotic mapping in the initialization of the algorithm to maintain the diversity of whale populations; introduced adaptive inertia weights in the updating of whale spiral positions to prevent the algorithm from falling into a local optimum; and introduced Lévy flight in the random search of whales, which improved the algorithm's global search capability. However, the algorithm introduces several new parameters, which need to be carefully

adjusted to obtain the best performance, increasing the difficulty of algorithm parameter adjustment. Reference [20] introduced cubic chaotic mapping initialization to enhance the traversal of the initial solution; introduced adaptive inertia weight coefficients and improved the convergence factor nonlinearly to balance the global search and local search ability; improved the spiral search equation so that the whale dynamically adjusts the search shape to enhance the algorithm's global search ability to break through the local optimum; and introduced a generalized reverse learning mechanism in order to enhance the algorithm's ability to jump out of the local optimum. Although the introduction of a variety of new parameters and mechanisms improves the performance of the algorithm, the computational complexity and cost of the algorithm inevitably increase. Reference [21] used a tent map function to optimize the distribution of the initial population in the problem domain; constructed the new iteration-based update strategies of convergence factor and inertia weight to regulate the balance between global and local search capabilities; and proposed an optimal feedback strategy in the prey search phase to enhance the global search capability. However, the optimal feedback strategy is more sensitive to the problem size, and it is necessary to analyze the problem size in advance to better utilize this strategy in practical applications. Reference [22] improved the compact algorithm using new parallel techniques for its shortcomings and combined it with the whale algorithm to propose a parallel compact based whale optimization algorithm. The algorithm has low memory consumption and strong local optimization jump-out ability, but it does not consider the ability to balance global optimization and local optimization. Reference [23], based on combining the whale optimization algorithm and the slime mold algorithm, improved the probability of the algorithm to obtain the global optimal solution by adjusting the dynamic parameters and introducing dynamic weights. However, no consideration is given to enhancing the diversity of the initial solution, which may cause the algorithm to fall into the local optimum.

For the frequency tracking control system of WPT, most scholars use the control method combining fuzzy rules and PI, and more complex ones combine neural networks, fuzzy rules and PI [24]. Although these control methods can greatly improve the effect of frequency tracking control, the complex controller will inevitably increase the design difficulty, and the debugging cycle will become longer, which is a big challenge for the researchers' energy and technology. As for the basic PI controller, although it is simple in structure, easy to implement, and can also obtain good control effect, but want to debug a set of appropriate parameters need to have sufficient experience. Intelligent algorithms can easily help us to optimize the parameters, which not only can have a good control effect, but also can save us a lot of time and energy. Therefore, this paper proposes an Improved Whale Optimization Algorithm (IWOA) to optimally adjust the PI parameters of frequency tracking control.

The contributions and structures of this paper are as follows:

(1) Aiming at the shortcomings of WOA, which is easy to fall into local optimum and slow convergence, this paper improves the algorithm in the following ways: firstly, the Kent chaotic mapping is used to initialize the whale population to improve the diversity of the initial solution; secondly, adaptive weighting coefficients are introduced and the convergence factor is nonlinearly improved to achieve the balance between the algorithm's global search and the local search ability; finally, the sine-cosine strategy and Cauchy reverse learning strategy are introduced to avoid the problem that the algorithm is prone to premature maturity.

(2) The improved algorithm is tested using eight benchmark test functions and evaluated using the Wilcoxon rank sum test, comparing with other mainstream algorithms to validate the capability of the proposed algorithm. The computational complexity of IWOA and WOA is also compared and briefly analyzed from the perspective of algorithm runtime using post hoc statistical methods.

(3) IWOA and WOA are applied to the frequency tracking control PI parameter tuning of the WPT system, and the frequency tracking control simulation is carried out to compare the phase difference curves under the control of different PI parameters and to verify the PI parameter tuning capability of IWOA.

II. SYSTEM MODELING AND ANALYSIS

A. MCR-WPT SYSTEM CIRCUIT MODELING

In this paper, the MCR-WPT system adopts a typical dual-coil S-S topology, as shown in Fig. 1, which mainly consists of a DC power supply, a full-bridge inverter circuit, resonant circuits at the transmitter and receiver, a full-bridge rectifier circuit and a load. Where U_d is the DC power supply; four IGBTs Q_1 to Q_4 constitute a full-bridge inverter; C_1 and C_2 are the resonance compensation capacitors corresponding to the transmitter and receiver; R_1 and R_2 are the parasitic resistors of the transmitter and receiver; L_1 is the inductance of the transmitter coil; L_2 is the inductance of the receiver coil; M is the mutual inductance between the transmitter coil and the receiver coil; the transmitter terminals D_1 to D_4 constitute the full-bridge rectifier, C_L is the rectifier bridge filter capacitor, R_L is the load resistance. The equivalent circuit model is shown in Fig. 2.

For the convenience of analyzing and calculating the system, Z_1 and Z_2 are denoted as the equivalent impedances of the transmitter and receiver, whose expressions are, respectively:

$$\begin{cases} Z_1 = R_1 + j\omega L_1 + \frac{1}{j\omega C_1} \\ Z_2 = R_2 + R_o + j\omega L_2 + \frac{1}{j\omega C_2} \end{cases} \quad (1)$$

Applying Kirchhoff voltage law (KVL), the voltage equations of the resonant circuit at the transmitter and receiver can

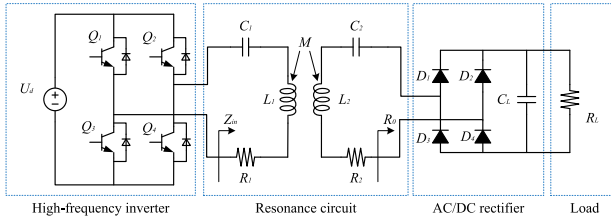


FIGURE 1. Main circuit structure of MCR-WPT with SS-type topology.

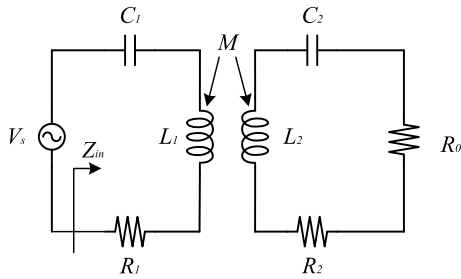


FIGURE 2. Equivalent circuit model.

be obtained as follows:

$$\begin{cases} I_1 Z_1 - V_s - j\omega M I_2 = 0 \\ I_2 Z_2 - j\omega M I_1 = 0 \end{cases} \quad (2)$$

where, ω is the angular frequency, I_1 is the current at the transmitter, I_2 is the current at the receiver, and V_s is the input voltage at the receiver.

The expression for the current at the transmitter and receiver can be found by Eq. (2) as:

$$\begin{cases} I_1 = \frac{Z_2 V_s}{Z_1 Z_2 + \omega^2 M^2} \\ I_2 = \frac{j\omega M V_s}{Z_1 Z_2 + \omega^2 M^2} \end{cases} \quad (3)$$

The equivalent input impedance Z_{in} of the system is calculated by Eq. (3) and expanded to obtain the expression as:

$$\begin{aligned} Z_{in} &= \frac{V_s}{I_1} = Z_1 + \frac{\omega^2 M^2}{Z_2} \\ &= \left(R_1 + j\omega L_1 + \frac{1}{j\omega C_1} \right) + \frac{\omega^2 M^2}{R_2 + R_o + j\omega L_2 + \frac{1}{j\omega C_2}} \end{aligned} \quad (4)$$

Eq. (4) can be rewritten as:

$$\begin{aligned} Z_{in} &= \left[R_1 + \frac{\omega^2 M^2 (R_2 + R_o)}{(R_2 + R_o)^2 + \left(\omega L_2 - \frac{1}{\omega C_2} \right)^2} \right] \\ &+ j \left[\omega L_1 - \frac{1}{\omega C_1} - \frac{\omega^2 M^2 \left(\omega L_2 - \frac{1}{\omega C_2} \right)}{(R_2 + R_o)^2 + \left(\omega L_2 - \frac{1}{\omega C_2} \right)^2} \right] \end{aligned} \quad (5)$$

The equivalent input impedance Z_{in} of the system is the ratio of the high-frequency inverter output voltage to the transmitter current, and the phase difference between the two can be obtained from Eq. (5). Since R_1 and R_2 are very small and can be ignored, the phase difference is expressed as:

$$\theta = \tan^{-1} \left[\frac{\left(\omega L_2 - \frac{1}{\omega C_2} \right)^2 + R_o^2}{\omega^2 M^2 R_o} \times \left(\omega L_1 - \frac{1}{\omega C_1} - \frac{\omega^2 M^2 \left(\omega L_2 - \frac{1}{\omega C_2} \right)}{\left(\omega L_2 - \frac{1}{\omega C_2} \right)^2 + R_o^2} \right) \right] \quad (6)$$

Analyzing Eq. (6) shows that when $\omega L - 1/\omega C = j\omega L + 1/j\omega C = 0$, the phase difference θ between the voltage and current at the transmitter is constant at 0, and the MCR-WPT system is in a resonant operating state. At this time, no matter how the load value changes, the phase difference does not change.

Based on the resonance condition, the detuning rate is defined as:

$$\gamma = \omega L - \frac{1}{\omega C} \quad (7)$$

When $\gamma = 0$, the system is in resonance state, the coil loop is purely resistive; when $\gamma > 0$, the system is in over-resonance state, the coil loop is inductive; when $\gamma < 0$, the system is in under-resonance state, the coil loop is capacitive.

According to Eq. (3) the input power P_{in} and output power P_{out} expressions of the system can be calculated as:

$$\begin{cases} P_{in} = V_s I_1 = \frac{Z_2 V_s^2}{Z_1 Z_2 + \omega^2 M^2} \\ P_{out} = I_2^2 R_o = \frac{\omega^2 M^2 V_s^2 R_o}{(Z_1 Z_2 + \omega^2 M^2)^2} \end{cases} \quad (8)$$

Based on Eq. (1), Eq. (7) and Eq. (8) the system transmission efficiency η expression can be calculated as:

$$\begin{aligned} \eta &= \frac{P_{out}}{P_{in}} = \frac{\omega^2 M^2 R_o}{Z_1 Z_2 + \omega^2 M^2 Z_2} \\ &= \frac{\omega^2 M^2 R_o}{(R_1 + j\gamma) \times (R_2 + R_o + j\gamma)^2 + \omega^2 M^2 (R_2 + R_o + j\gamma)} \end{aligned} \quad (9)$$

From Eq. (9), it can be seen that when the system is in the resonant state, the coil circuit equivalent impedance is the smallest, the coil energy can realize the maximum efficiency of transmission. When the system is working in the detuned state, the equivalent circuit impedance is inductive or capacitive. At this time, part of the power in the transmission process will be consumed to do useless work, the transmission efficiency of the system will be greatly reduced.

B. FREQUENCY TRACKING CONTROL SYSTEM

From the modeling analysis of the MCR-WPT system in the previous section, it can be seen that during the operation of the system, the operating frequency of the inverter output is required to be consistent with the intrinsic resonance frequency of the system, so that the phase difference between the voltage and the current at the transmitter is 0, and the maximum efficiency is maintained for energy transfer. In order to realize this purpose, an effective detuning control method should be implemented. In this paper, the frequency tracking control method controlled by PI controller is selected, which is simple in structure, easy to implement and effective. The control system block diagram is shown in Fig. 3.

The frequency tracking control system consists of current acquisition module, phase detector, PI controller, voltage controlled oscillator (VCO) and pulse generator. First, the phase detector is used to obtain the phase difference $\Delta\theta$ between the voltage and the current signals. $\Delta\theta$ is used as the error signal to output the frequency f through the PI controller. Then the VCO outputs the waveform u with the same frequency according to the f , and then the pulse generator generates the corresponding PWM to drive the inverter, so as to control the frequency of the output voltage of the inverter, making the voltage and current have a phase difference of 0, so that the MCR-WPT system can work in a resonant state.

III. IMPROVED WHALE OPTIMIZATION ALGORITHM

The principle of PI controller is simple and the control effect is good, however, the control parameter plays a decisive role in the control performance. To debug a suitable set of parameters requires personnel with sufficient experience. Intelligent optimization algorithms can help us to find out the optimal result of the problem within the given range. In this paper, we propose to use the improved whale optimization algorithm to optimize and tune the PI controller. Aiming at the problems of the standard whale optimization algorithm, such as slow convergence speed and easy to fall into local optimization, this paper proposes an improved whale optimization algorithm that incorporates four strategies.

A. STANDARD WHALE OPTIMIZATION ALGORITHM

The Whale Optimization Algorithm is a new heuristic optimization algorithm based on the principle of humpback whale feeding behavior. In WOA, each feasible solution is represented by the position of a humpback whale. Each whale has two behaviors during the hunting process: one is the encircling prey behavior in which all the whales approach the prey; the other is the bubble net behavior in which the whales swim in a circle and emit bubbles to repel the prey. Whales randomly adopt one of the two behaviors to hunt prey in each generation of swimming. When whales hunt, they randomly choose to swim to whales in the best position or to whales in a random position.

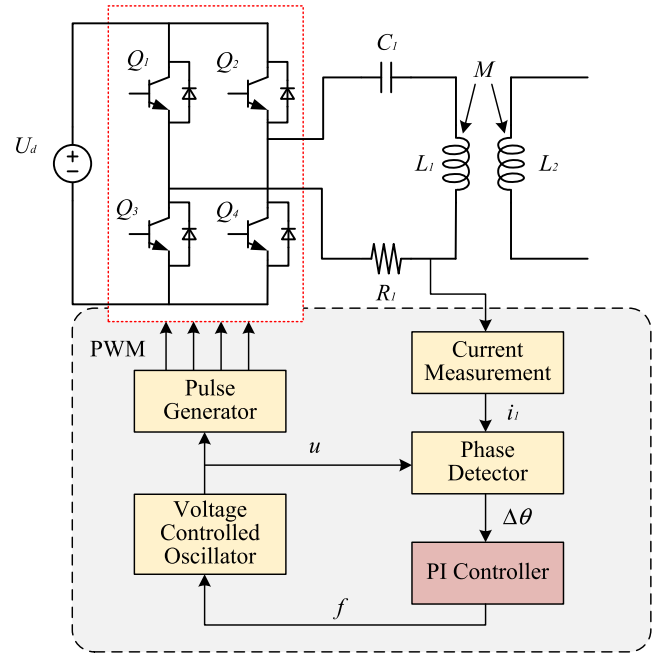


FIGURE 3. Block diagram of MCR-WPT frequency tracking control system.

1) ENCIRCLING PREY

To describe the behavior of humpback whales around their prey during feeding, the following mathematical model is proposed:

$$\vec{D}_1 = \left| \vec{C} \cdot \vec{X}^*(t) - \vec{X}(t) \right| \quad (10)$$

$$\vec{X}(t+1) = \vec{X}^*(t) - \vec{A} \cdot \vec{D}_1 \quad (11)$$

where \vec{D}_1 is the distance between the individual whale and the prey, t is the current number of iterations, $\vec{X}^*(t)$ is the current best position of the whale, and $\vec{X}(t)$ is the current position vector of the whale. \vec{A} and \vec{C} are coefficients, calculated as follows:

$$\vec{A} = 2 \cdot \vec{a} \cdot \vec{r}_1 - \vec{a} \quad (12)$$

$$\vec{C} = 2 \cdot \vec{r}_2 \quad (13)$$

$$\vec{a} = 2 - \frac{2t}{T_{\max}} \quad (14)$$

where \vec{r}_1 and \vec{r}_2 are random vectors in $[0, 1]$, the value of \vec{a} decreases from 2 to 0 in a linear fashion, and T_{\max} is the maximum number of iterations.

2) HUNTING FOR PREY

Based on the humpback whale's hunting style, its prey hunting behavior is represented in a mathematical model as:

$$\vec{D}_2 = \left| \vec{X}^*(t) - \vec{X}(t) \right| \quad (15)$$

$$\vec{X}(t+1) = \vec{D}_2 \cdot e^{bl} \cdot \cos(2\pi l) + \vec{X}^*(t) \quad (16)$$

where \vec{D}_2 is the distance between the individual whale and its prey, b is a constant, and l is a random number with values in the range $[-1, 1]$.

The whale swims in a spiral pattern toward its prey while simultaneously narrowing its envelope. Assume that the probability of choosing the mechanism of narrowing the encirclement is p , and the probability of choosing the spiral to update the whale's position is $1 - p$. The mathematical description of this synchronized behavior is as follows:

$$\vec{X}(t+1) = \begin{cases} \vec{X}^*(t) - \vec{A} \cdot \vec{D}_1 & p < 0.5 \\ \vec{D}_2 \cdot e^{bl} \cdot \cos(2\pi l) + \vec{X}^*(t) & p \geq 0.5 \end{cases} \quad (17)$$

A decreasing value of \vec{a} is set near the prey, and \vec{a} is a linearly varying parameter, so that when attacking the prey, the magnitude of fluctuation of \vec{A} decreases as \vec{a} decreases. During the iteration process, when the value of \vec{a} decreases from 2 to 0, \vec{A} is any random value in $[-a, a]$. When \vec{A} is $[-1, 1]$, the new position of an individual whale can be defined anywhere in between the current position of the individual whale and the position of prey. The algorithm sets the condition that the whale launches an attack on the prey as $A < 1$.

3) SEARCHING FOR PREY

The mathematical model when searching for prey is as follows:

$$\vec{D}_3 = \left| \vec{C} \cdot \vec{X}_{rand}(t) - \vec{X}(t) \right| \quad (18)$$

$$\vec{X}(t+1) = \vec{X}_{rand}(t) - \vec{A} \cdot \vec{D}_3 \quad (19)$$

where \vec{X}_{rand} is the position of the randomly selected whale and \vec{D}_3 is the distance of the randomly selected individual whale from the prey.

When $A \geq 1$, an individual whale is randomly selected, and the position update is performed by replacing the current whale position with the randomly selected whale position, which causes the whale to deviate from the prey and thus find a more suitable prey.

B. IMPROVED WHALE OPTIMIZATION ALGORITHM

1) KENT CHAOTIC MAPPING INITIALIZATION

The population initialization of the standard WOA is to randomly generate the positions of individual whales within the upper and lower bounds, and such an initialization may cause the whales to be unevenly distributed in terms of their positions in the space, leading to the algorithm maturing prematurely and falling into local optimum solutions. In order to solve this problem, this paper adopts an initialization method based on Kent chaotic sequences, which has better traversal properties compared to the classical logistic mapping [25].

Due to the properties of chaotic mapping such as randomness and traversal, it can be used in the initialization of intelligent algorithm population. The principle is to use

chaotic mapping to generate sequences between $[0, 1]$, and then initialize the whale population according to the chaos factor. This can make the distribution of whales more reasonable and uniform at the beginning and avoid premature maturity. The mathematical model of Kent mapping is shown in Eq. (20):

$$x_{n+1} = \begin{cases} \frac{x_n}{a} & 0 < x_n \leq a \\ \frac{1-x_n}{1-a} & a < x_n < 1 \end{cases} \quad (20)$$

where a is the tuning parameter of the Kent mapping, $a \in (0, 1)$. The model initialized using chaotic mapping is shown in Eq. (21):

$$x = x_{\min} + Chaos \times (x_{\max} - x_{\min}) \quad (21)$$

where x_{\min} and x_{\max} are the lower and upper bounds on the values of the independent variables, $Chaos$ is the chaos factor generated by the Kent mapping, and x is the position of the individual mapped into the search space.

2) ADAPTIVE WEIGHTING COEFFICIENT AND IMPROVED CONVERGENCE FACTOR

From the analysis of WOA, it can be seen that the convergence factor \vec{a} is crucial for balancing the algorithm's global and local search ability, and the positional changes between individuals in the population are also related to it. However, the convergence factor \vec{a} in WOA decreases linearly from 2 to 0 as the number of iterations increases, which makes the iteration speed of the algorithm slower; at the same time, when the algorithm performs local optimization, the search agent can only be close to the local optimum solution, and cannot perform better local optimization. To address the above problems, this paper improves the convergence factor \vec{a} and introduces the adaptive weight coefficient ω , which is formulated as follows:

$$a = -\cos\left(\frac{\pi t}{Max_{iter}} + \pi\right) + 1 \quad (22)$$

$$w = k \cos\left(\frac{d\pi t}{Max_{iter}}\right) \quad (23)$$

where t is the current number of iterations, Max_{iter} is the maximum number of iterations, and k and d are the adjustment coefficients.

Because the cosine function has the characteristic of periodically decreasing from 1 to -1, Eq. (22), compared with the linear iteration of the original algorithm, the convergence factor can decrease nonlinearly from 2 to 0. Similarly, Eq. (23) makes the weights decrease nonlinearly from 1 to 0. The adaptively adjusted WOA maintains a large weight at a small iteration rate in the early stage of the iteration, which can increase the algorithm's global searching ability; the weight drops rapidly after a certain iteration to improve the searching accuracy in the later stage of the iteration, thus realizing the balance between the global searching ability and the local searching ability of the algorithm. After a certain number of

iterations, the weight decreases rapidly, which improves the optimization accuracy at the later stage of iteration, thus realizing the balance between the global and local optimization ability of the algorithm. After the introduction of adaptive adjustment strategy, Eq. (11), Eq. (16) and Eq. (19) are updated as follows:

$$\vec{X}(t+1) = w\vec{X}^*(t) - \vec{A} \cdot \vec{D}_1 \quad (24)$$

$$\vec{X}(t+1) = \vec{D}_2 \cdot e^{bl} \cdot \cos(2\pi l) + w\vec{X}^*(t) \quad (25)$$

$$\vec{X}(t+1) = w\vec{X}_{rand}(t) - \vec{A} \cdot \vec{D}_3 \quad (26)$$

3) FUSION OF SINE-COSINE ALGORITHM STRATEGY

Sine cosine algorithm (SCA) mainly utilizes the mathematical properties of sine and cosine functions to achieve the purpose of finding the optimal solution through iteration. In SCA, it is assumed that the individuals in the population of t -th generation are $X_i^t = (x_{i1}^t, x_{i2}^t, \dots, x_{iD}^t)$, where $i = 1, 2, \dots, N$, N is the population size and D is the individual dimension. The algorithm generates the positions of N populations randomly in the space, calculates the fitness value of each individual, and saves the optimal position and its corresponding fitness value by sorting the fitness value to store the best. The individual updates the position in the manner shown in Eq. (27):

$$X_d^i(t+1) = \begin{cases} X_d^i(t) + a \times \sin(r_3) \times |r_4 X^* - X_d^i(t)|, & r_5 < 0.5 \\ X_d^i(t) + a \times \cos(r_3) \times |r_4 X^* - X_d^i(t)|, & r_5 \geq 0.5 \end{cases} \quad (27)$$

where $X_d^i(t)$ is the position component of the i -th individual in the d -th dimension of the t -th generation, X^* is the current optimal position, r_3 is a random number between $[0, 2\pi]$, r_4 is a random number between $[0, 2]$, and r_5 is a random number between $[0, 1]$, and the parameter a is the same as that of Eq. (22), which is used for controlling the search direction.

Considering that in WOA, the position of the individual with the best fitness value is assigned to the leader of the whale group at each iteration, in such a way that the algorithm is prone to fall into local optimum, resulting in lower optimization accuracy. In SCA, on the other hand, the algorithm can randomly select the sine-cosine cross-searching optimization, which makes the updating methods of the positions complement each other, and better coordinates the global optimization and local optimization ability, so that SCA gradually shrinks and hovers around the target solution.

Therefore, in the IWOA proposed in this paper, the leader that has been sorted to survive the optimization is not directly proceeding to the next iteration process. Instead, the current leader position is recorded, and at the same time, the position of each individual in the population is updated with the sine-cosine position according to Eq. (27). Then the fitness value of each individual is calculated and a greedy mechanism is introduced to filter a new leader position by

comparing the fitness. Finally, the current optimal individual whale position is updated by comparing the size of the fitness value between the leader before the sine-cosine operation and the new leader.

4) FUSION OF CAUCHY REVERSE LEARNING STRATEGY

Suppose $P = x(x_1, x_2, \dots, x_k)$ is a point in k -dimensional space, where $x_i \in [a_i, b_i]$, $i = 1, 2, \dots, k$, and a_i and b_i are the minimum and maximum values of the point P in the i -th dimension, then the reverse point of the point P is:

$$OP = \bar{x}(\bar{x}_1, \bar{x}_2, \dots, \bar{x}_k) \quad (28)$$

where $\bar{x}_i = a_i + b_i - x_i$.

The above are the basic concepts and mathematical formulas for reverse points in general. There are many novel concepts of reverse points that have arisen, and among them the mathematical formula of the Cauchy reverse point is as follows:

$$QOP = \text{rand} \left(\frac{a_i + b_i}{2}, a_i + b_i - x_i \right), i = 1, 2, \dots, k \quad (29)$$

Compared with the ordinary reverse point, the Cauchy reverse point is a randomly generated point between the midpoint and the ordinary reverse point. In the IWOA proposed in this paper, the Cauchy reverse jump method is also used to generate the reverse population of the current population according to Eq. (29), and then merge the two populations. The fitness of all individuals is calculated and then sorted, and half of the individuals with better fitness are selected to enter the next iterative loop, thus speeding up the convergence of the algorithm. The Cauchy reverse jump method is defined as: if $\text{rand} \leq Jr$, the Cauchy reverse population of the current population is generated. Where Jr is the jump rate, which is used to control the weight of executing the Cauchy reverse learning strategy during the iteration of the algorithm; rand is a random number between $[0, 1]$.

C. FLOWCHART OF IWOA

Based on the above four improvement strategies, the IWOA flowchart proposed in this paper is shown in Fig. 4, and the specific implementation steps are described as follows:

Step1: Set the initial parameters, including the population size N , the maximum number of iterations T_{\max} , and the upper and lower limits of the solution space;

Step2: Kent chaotic mapping is used to initialize the whale population according to Eq. (20) and Eq. (21);

Step3: Calculate the fitness of each individual whale and record the current optimal individual whale and its position;

Step4: When the current iteration number is less than the maximum iteration number, calculate the parameter \vec{a} according to Eq. (22), calculate the parameter ω according to Eq. (23), update A and C , and generate a random number p ;

Step5: If the random number $p \geq 0.5$, update the position of whale population according to Eq. (25); otherwise, determine whether $|A|$ is less than 1. If $|A| < 1$, update the position of

whale population according to Eq. (24), and if $|A| \geq 1$, update the position of whale population according to Eq. (26);

Step6: Update the position of each whale individual in the population according to Eq. (27), calculate the fitness value, filter a new optimal whale individual by comparison, and introduce a greedy mechanism to decide whether the current optimal whale individual and its position need to be updated;

Step7: If $\text{rand}[0, 1] \leq Jr$, generate the reverse population of the current population according to Eq. (29) and merge them, calculate the fitness of all individuals, sort them, take the whale individual with the optimal fitness value as the global optimal solution, and select half of the individuals with better fitness to enter the next iteration of the loop;

Step8: Determine whether the number of iterations reaches the maximum number of iterations T_{\max} , if it meets, then output the global optimal solution; otherwise return to Step4 to continue iteration.

The pseudocode is shown in Algorithm 1.

IV. EXPERIMENTS AND RESULTS ANALYSIS

The simulation experiments in this chapter are divided into three parts. The first is the algorithm performance test of the IWOA proposed in this paper, and eight benchmark test functions are selected to be used for testing and evaluating the optimization ability of the IWOA. The second is the analysis of some simulations of the MCR-WPT system. The third is the application of the IWOA to the PI Parameters optimization of the frequency tracking control system.

The running environment for all the experiments in this paper is 64 for Windows 11, the CPU type is AMD Ryzen 7 5800H with 3.2GHz, the main memory is 16G, and the programming software is MATLAB R2020b.

A. ALGORITHM PERFORMANCE TESTING AND ANALYSIS

The experiments in this section select eight benchmark test functions. As shown in Table 1, F1-F5 are single-peak functions, where the local optimum of the function is the global optimum of the function, which is usually used to test the convergence speed of the algorithm and the accuracy of the optimization search; F6-F8 are multi-peak functions, which have multiple local optimums, and are usually used to test the ability of the algorithm to jump out of the local optimum and explore the global.

In order to verify the effectiveness of the algorithm, two classical population optimization algorithms, PSO and GWO, are selected for experiments with the standard WOA as well as the IWOA proposed in this paper. To reduce experimental chance, the four algorithms are subjected to 30 independent experiments for each test function and the performance of the algorithms is analyzed by the optimal value, average value and standard deviation. The algorithm parameters set in the experiment are: population size $N=30$, maximum number of iterations $T=200$, and other specific parameters are shown in Table 2. After 30 independent experiments were completed, the results were subjected to data processing, and the specific experimental data are shown in Table 3.

Algorithm 1 The pseudocode of IWOA

```

1: Set the initial parameters
2: Kent chaotic mapping is used to initialize the whale population
3: Calculate the fitness of each individual whale and record the current optimal individual as the first whale optimal individual  $X_i(t)$ 
4: while ( $T < T_{\max}$ )
5:   for ( $i = 0; i < N; i++$ )
6:     Update a, w, A, C, p
7:     if1 ( $p < 0.5$ )
8:       if2 ( $|A| < 1$ )
9:         Update position by Equation (25)
10:      else if2
11:        Update position by Equation (27)
12:      end if2
13:    else if1 ( $p \geq 0.5$ )
14:      Update position by Equation (26)
15:    end if1
16:    Perform sine-cosine calculation on all whale individuals, filter out a new optimal individual, and record it as the second whale optimal individual  $X_i(t)'$ .
17:    if3 ( $F(X_i(t)) < F(X_i(t)')$ )
18:      Retain the first optimal individual  $X_i(t)$  as the whale leader.
19:    else if3
20:      Replace  $X_i(t)$  with the second optimal individual  $X_i(t)'$  and update it to be the new whale leader
21:    end if3
22:  end for
23:  if4  $\text{Rand}[0,1] \leq Jr$ 
24:    Generate Cauchy reverse population QOP of current population P
25:    Half of the individuals with better fitness are selected to enter the next iterative loop and use the individual with the optimal fitness as the current optimal solution
26:  else if4
27:    Keep the current population into the next loop
28:  end if4
29:   $T=T+1$ 
30: end while
31: End of the algorithm, output the global optimal solution

```

From Table 3, it can be seen that in terms of the single-peak functions F1-F5, IWOA has the strongest ability to find the optimal solution among the four algorithms. It is able to find the optimal solution in a faster and more stable way. For functions F1 and F3, IWOA found the optimal solution 0 and the average value is also 0. This shows that IWOA can find the optimal solution in almost every one of the 30 experiments, and the ability of finding the optimal solution is obviously stronger than the other three functions; For functions F2 and F4, although IWOA does not find the optimal solution, the average values are 6.78E-219 and 6.10E-214, respectively,

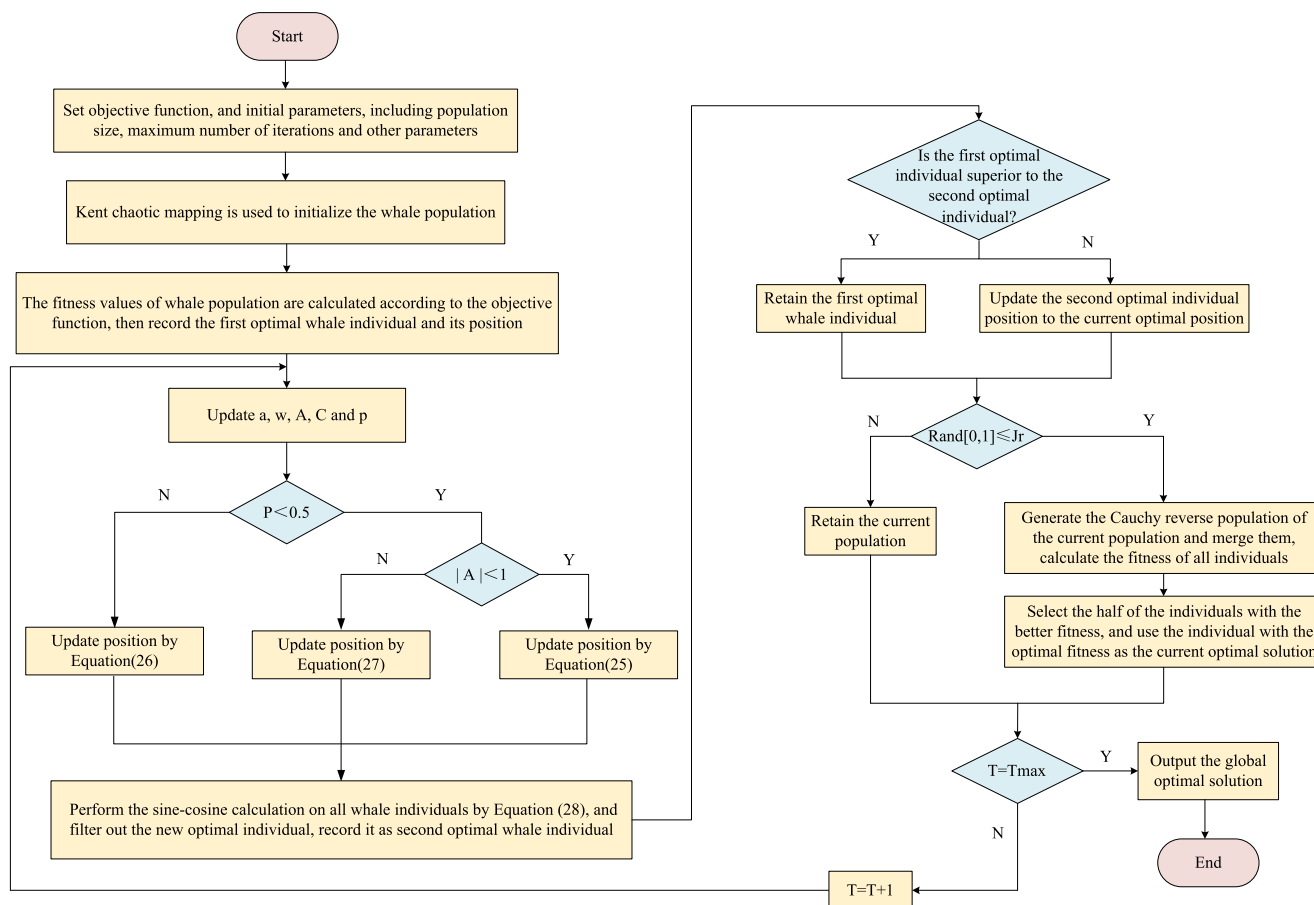


FIGURE 4. The flowchart of IWOA.

which are more than 200 orders of magnitude different from the average values of the other three algorithms. It also proves that IWOA has the strongest ability to find the optimal solution; For function F5, the average of the IWOA solution results is slightly stronger than the other three algorithms, despite the fact that the difference between them and WOA and GWO is not very large. Overall, the experiments demonstrate that the IWOA proposed in this paper has good optimization ability and convergence accuracy.

And for the multi-peak functions F6-F8, similarly, both IWOA and WOA find optimal solutions for functions F6 and F8, and the average value of IWOA is 0, which illustrates that IWOA finds the optimal solution almost every time; Although IWOA does not find the optimal solution of function F7, and the average result is not much different from that of WOA, it has the smallest standard deviation, which shows the stability and the ability to jump out of the local optimum of IWOA. Overall, the experiments demonstrate that the IWOA proposed in this paper has better global search capability and the ability to avoid falling into local optimum.

In order to visualize and analyze the algorithm’s optimization searching effect, the convergence curves of the four algorithms on the eight benchmark test functions are given in Fig. 5~12. Among them, Fig. 5~9 shows the convergence

TABLE 1. Test function.

Function number	Name	Dim	Search space	Optimal value
F1	Sphere	30	[-100, 100]	0
F2	Schwefel2.22	30	[-10, 10]	0
F3	Schwefel1.2	30	[-100, 100]	0
F4	Schwefel2.21	30	[-100, 100]	0
F5	Quartic	30	[-1.28, 1.28]	0
F6	Rastrigin	30	[-5.12, 5.12]	0
F7	Ackley	30	[-32, 32]	0
F8	Griewank	30	[-600, 600]	0

curves of single-peak functions F1-F5; Fig. 10~12 shows the convergence curves of multi-peak functions F6-F8. As can be seen from these figures, the convergence speed and convergence accuracy of IWOA are significantly better than the other algorithms. This is due to the fact that the algorithm incorporates Kent chaotic mapping, the improved convergence factor, the adaptive weighting coefficient, as well as the sine-cosine strategy and the Cauchy reverse learning strategy, so that the convergence speed and the solution accuracy of IWOA are better than other algorithms.

TABLE 2. Parameter settings of algorithms used in experiments.

Algorithm	Population	Iteration	Others
PSO	30	200	$C_1 = C_2 = 2, \omega = [0.6, 0.9]$
GWO	30	200	a decreases linearly from 2 to 0
WOA	30	200	$b=1, a$ decreases linearly from 2 to 0
IWOA	30	200	$k=2, d=0.5, b=1, Jr=0.95$

To further demonstrate the performance of the improved algorithm, this paper uses Wilcoxon rank sum test to evaluate the proposed improved algorithm. Statistical tests are used at 5% significant level to verify whether the results of each run of the proposed improved algorithm in this paper are statistically significantly different from other algorithms. Usually, when $p < 5\%$, it can be considered as a strong validation of the rejection of the null hypothesis, indicating that the two compared algorithms are significantly different.

Table 4 lists the p-values of this paper’s proposed IWOA with the other three compared algorithms in Wilcoxon test under eight test functions. Where $p_1, p_2,$ and p_3 denote the p-values of IWOA with WOA, GWO, and PSO, respectively, and “+”, “=”, and “-” indicate that the performance of IWOA is better than, equal to and inferior to the compared algorithms, respectively. The analysis of the results in Table 4 shows that the p-values of IWOA are basically much less than 5%, which indicates that the performance of the algorithm proposed in this paper is statistically significantly better, and further proves that the improved algorithm in this paper has a stronger performance of optimality seeking.

It is easy to see that IWOA incorporates a variety of strategies and the algorithm performance is more superior. However, due to the fact that the algorithms in the sine-cosine and Cauchy reverse strategy sessions will again solve for whale population position and fitness, this leads to the unavoidable fact that the computational complexity of the IWOA is higher compared to the original WOA. Therefore, in this paper, IWOA and WOA were compared and analyzed from the perspective of algorithmic running time on the F1 test function. Similarly, in order to reduce the experimental chance, 30 independent experiments are conducted on the function under each condition and the average running time is calculated. Table 5 shows the running time of the algorithms for the same number of maximum iterations and growth in population size, and Table 6 shows the running time of the algorithms for the same population size and growth in maximum iterations. Figures 13 and 14 show line graphs corresponding to Tables 5 and 6, respectively.

It can be seen that under the same conditions, the running time of IWOA is longer than that of WOA, and the running time of IWOA grows more with the linear increase of the population size and the maximum number of iterations, which verifies the previous conjecture. Although the introduction of the sine-cosine strategy and Cauchy reverse

TABLE 3. Comparison of the results of different algorithms.

Function	Index	PSO	GWO	WOA	IWOA
F1	Opt.	5.21E+00	4.26E-10	1.28E-35	0.00E+00
	Avg.	1.29E+01	1.02E-08	1.81E-27	0.00E+00
	Std.	3.84E+00	2.17E-08	7.89E-27	0.00E+00
F2	Opt.	8.12E+00	1.46E-06	1.34E-24	1.77E-232
	Avg.	1.42E+01	5.09E-01	5.26E-20	6.78E-219
	Std.	2.84E+00	2.74E+00	9.62E-20	0.00E+00
F3	Opt.	3.79E+02	3.76E-01	5.23E+04	0.00E+00
	Avg.	6.44E+02	4.07E+00	7.95E+04	0.00E+00
	Std.	2.03E+02	7.22E+00	2.05E+04	0.00E+00
F4	Opt.	2.19E+00	9.91E-03	3.02E+00	5.38E-231
	Avg.	3.09E+00	3.33E-02	6.40E+01	6.10E-214
	Std.	4.39E-01	2.21E-02	2.43E+01	0.00E+00
F5	Opt.	1.51E+01	1.27E-03	2.06E-04	1.95E-05
	Avg.	5.81E+01	6.84E-03	7.62E-03	3.14E-04
	Std.	2.77E+01	3.51E-03	7.89E-03	3.71E-04
F6	Opt.	1.76E+02	4.22E+00	0.00E+00	0.00E+00
	Avg.	2.45E+02	1.45E+01	7.58E-15	0.00E+00
	Std.	2.57E+01	4.67E+00	0.00E+00	0.00E+00
F7	Opt.	3.17E+00	6.06E-06	8.88E-16	8.88E-16
	Avg.	4.11E+00	1.74E-05	2.22E-14	8.88E-16
	Std.	3.45E-01	1.16E-05	1.46E-14	3.94E-31
F8	Opt.	5.56E-01	1.28E-09	0.00E+00	0.00E+00
	Avg.	7.82E-01	5.35E-03	3.86E-02	0.00E+00
	Std.	7.50E-02	1.08E-02	1.48E-01	0.00E+00

strategy will strengthen the algorithm’s superiority seeking ability, it has many more solution steps, and the complexity of the algorithm’s computation will undoubtedly be higher. Therefore, how to balance the superior optimization ability and the lengthy solution time is a problem worth thinking about. For the IWOA proposed in this paper, the parameters of appropriate population size and maximum iterations can be set to minimize the impact of computational complexity.

B. SIMULATION AND ANALYSIS OF MCR-WPT

In the MATLAB/Simulink simulation environment, the MCR-WPT system is modeled according to Fig. 1. In order to facilitate the simulation study, the electrical parameters of the MCR-WPT are designed specifically as shown in Table 7.

When no frequency tracking control method is used and the operating frequency is set to 70 kHz, the curves of voltage and current at the transmitter can be obtained. As shown in Fig. 15 and Fig. 16, Fig. 15 illustrates the curves of voltage

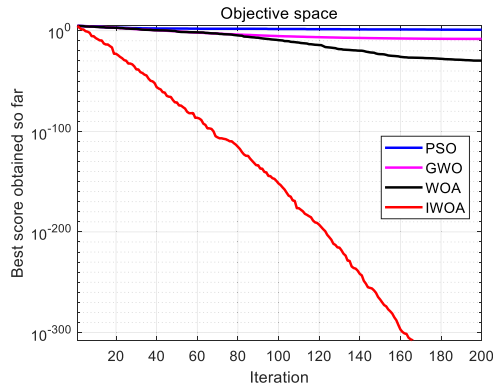


FIGURE 5. Convergence curve of F1.

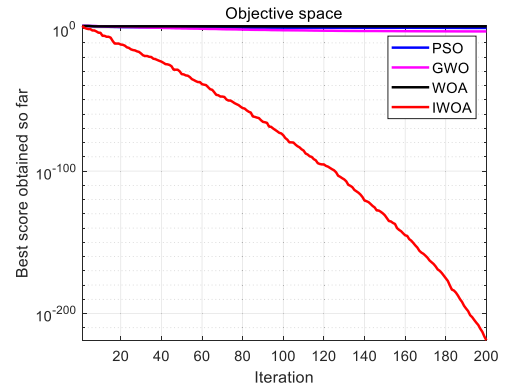


FIGURE 8. Convergence curve of F4.

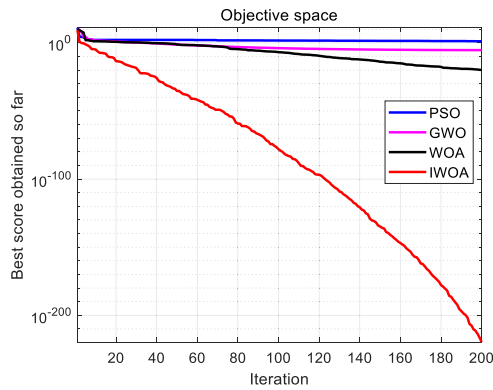


FIGURE 6. Convergence curve of F2.

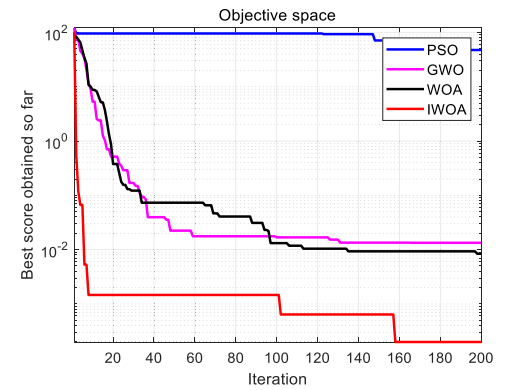


FIGURE 9. Convergence curve of F5.

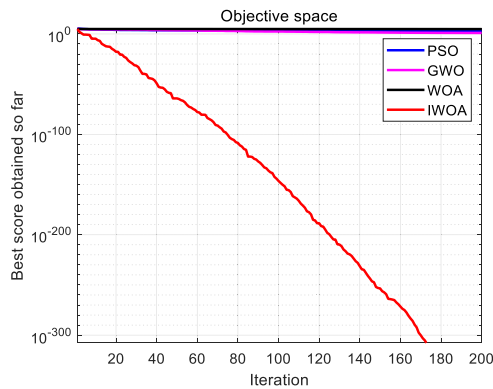


FIGURE 7. Convergence curve of F3.

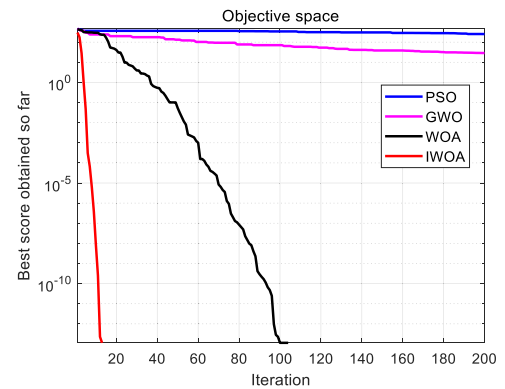


FIGURE 10. Convergence curve of F6.

and current at the transmitter, and Fig. 16 illustrates the curves of energy transfer efficiency of the system. When the system reaches stability, it is obvious that there is a large phase difference between the voltage and current at the transmitter. At this time, the MCR-WPT system does not work in a resonant state, and the energy transfer efficiency is only about 14%. This shows that frequency tracking control is very necessary.

When the frequency tracking control system was added, the PI Parameters were set to $P=2000$ and $I=800000$ by the trial-and-error method. The voltage and current curves at the transmitter are shown in Fig. 17. It can be found that

the voltage and current are in the same frequency and phase state, and the current value is also increased compared with Fig. 15. At this time, the MCR-WPT operates in a resonant state, which ensures that the system operates in high transmission efficiency. The frequency curve is given in Fig. 18, and it can be found that the frequency is finally stabilized at 77.4 kHz, which indicates that the resonant frequency of the system is 77.4 kHz. The energy transfer efficiency curve of the MCR-WPT with frequency tracking control is given in Fig. 19, and the transfer efficiency is stabilized at 75% after 0.01s. Compared with Fig. 16, the transmission

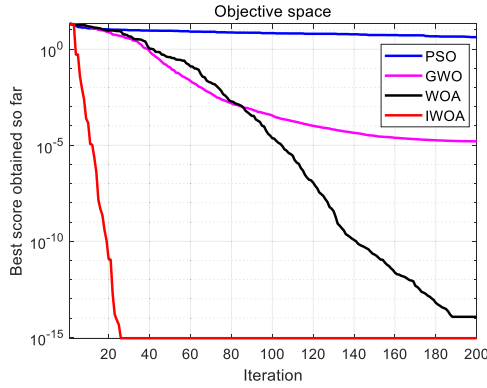


FIGURE 11. Convergence curve of F7.

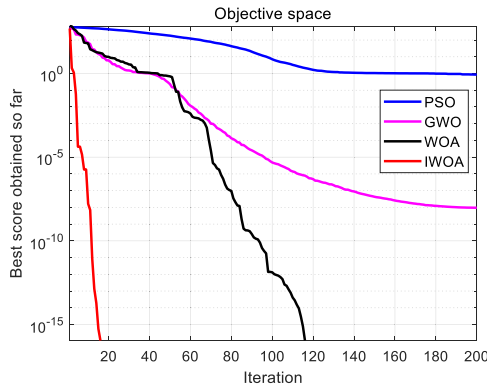


FIGURE 12. Convergence curve of F8.

TABLE 4. Wilcoxon rank sum test p value.

Function number	p_1	p_2	p_3
F1	1.73e-06	1.73e-06	1.73e-06
F2	1.73e-06	1.73e-06	1.73e-06
F3	1.73e-06	1.73e-06	1.73e-06
F4	1.73e-06	1.73e-06	1.73e-06
F5	2.12e-06	1.73e-06	1.73e-06
F6	3.12e-02	1.73e-06	1.73e-06
F7	1.58e-06	1.73e-06	1.73e-06
F8	2.50e-01	1.73e-06	1.73e-06
+/-/-	7/0/1	8/0/0	8/0/0

efficiency of the MCR-WPT with frequency tracking control is significantly improved.

However, when the PI Parameters are tuned by the trial-and-error method, it is usually inefficient and cannot ensure that the parameters obtained have a good control effect. Therefore, this paper proposes to use the IWOA optimization algorithm to optimally tune the frequency tracking control PI Parameters.

C. FREQUENCY TRACKING CONTROL SYSTEM WITH IWOA-PI TUNING

In control systems, an error integration criterion is often utilized to measure the excellence of control system performance. The error integration criteria include Integral Square Error criterion (ISE), Integral of Time and Square Error

TABLE 5. Running time of the algorithm (Max_iteration=200).

Population Size	Running time of WOA(s)	Running time of IWOA(s)
30	0.047	0.098
60	0.061	0.153
90	0.076	0.199
120	0.09	0.246
150	0.104	0.285

TABLE 6. Running time of the algorithm (population size =30).

Population Size	Running time of WOA(s)	Running time of IWOA(s)
200	0.047	0.098
400	0.061	0.152
600	0.077	0.199
800	0.092	0.247
1000	0.106	0.299

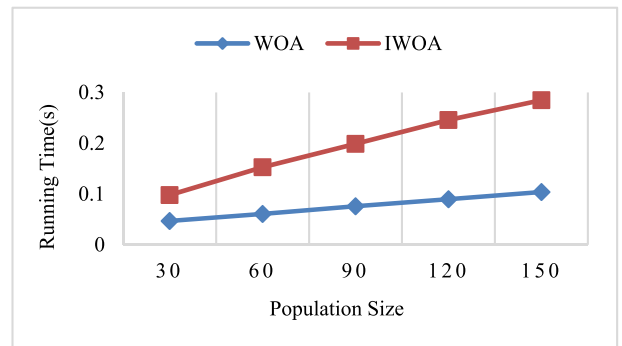


FIGURE 13. Running time curve (Max_iteration=200).

criterion (ITSE), Integral Absolute Error criterion (IAE) and Integral of Time and Absolute Error criterion (ITAE). ITAE is the absolute value of the error multiplied by time and integrated over time. It can reflect both the magnitude of the error (control accuracy) and the speed of convergence of the error, taking into account the control accuracy and convergence speed, and is suitable for judging the performance of the frequency tracking control system. The specific mathematical formula for ITAE is:

$$ITAE = \int_0^{\infty} t |e(t)| dt \quad (30)$$

The objective function of the IWOA in this paper mainly considers the control performance of the frequency tracking control system, so the objective function is established according to Eq. (30), where $e(t)$ is the phase difference between the voltage and current at the transmitter. IWOA searches for the optimal solution of the PI Parameters of the frequency tracking control system according to the objective function, and its specific schematic diagram is shown in Fig. 20.

After setting the initial parameters, the algorithm starts to run. each individual whale position generated by IWOA represents a set of PI control parameters, which are substituted

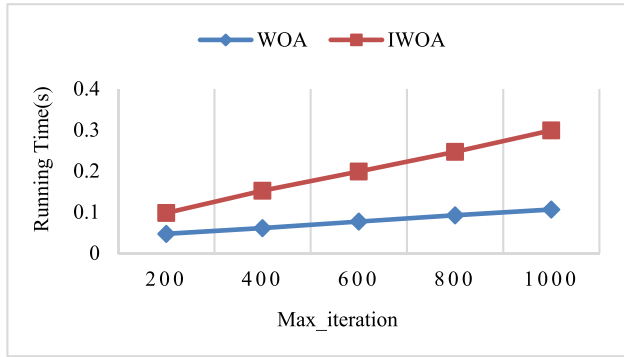


FIGURE 14. Running time curve (population size =30).

TABLE 7. Electrical parameters of the MCR-WPT.

Parameter	Value	Parameter	Value
U_d / V	24	R_2 / Ω	0.1
C_1 / nF	40	$L_1 / \mu H$	100
C_2 / nF	35	$L_2 / \mu H$	100
R_1 / Ω	0.1	R_L / Ω	20
$C_L / \mu F$	100	$M / \mu H$	20

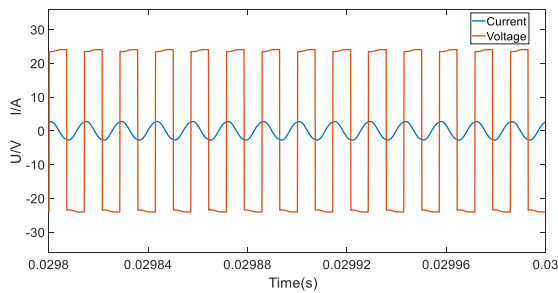


FIGURE 15. Voltage and current curves at the transmitter without frequency tracking control.

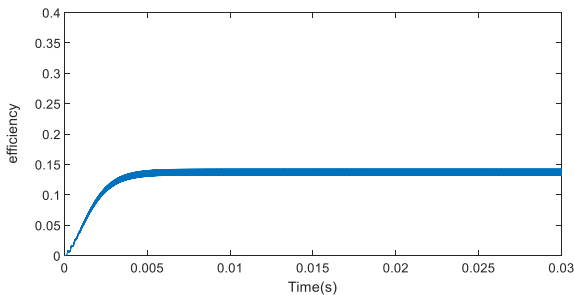


FIGURE 16. Efficiency of MCR-WPT without frequency tracking control.

into the control model for simulation. Then the fitness value of each individual whale is calculated based on the objective function, and the fitness value is returned to the algorithm for optimal fitness update. Repeated iterations are performed to update the individual whale position and optimal fitness until the maximum number of iterations is reached, and finally the optimal controller parameters are output.

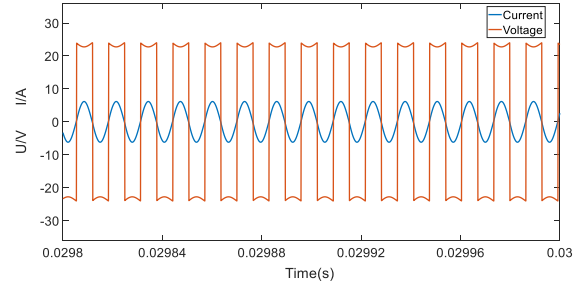


FIGURE 17. Voltage and current curves at the transmitter with frequency tracking control.

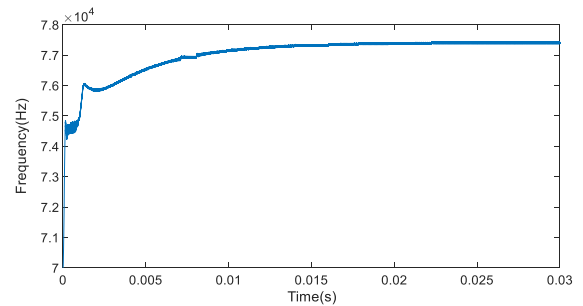


FIGURE 18. The resonant frequency with frequency tracking control.

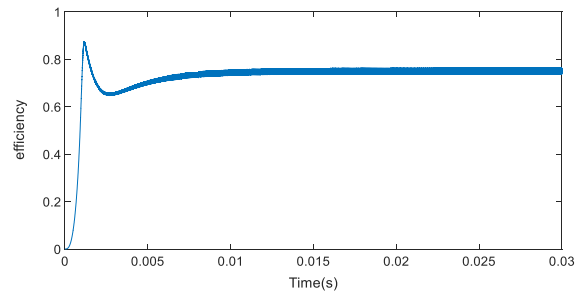


FIGURE 19. Transmission efficiency of MCR-WPT with frequency tracking control.

TABLE 8. Parameters of PI controller.

Parameter	WOA	IWOA
P	1843.8709974	1304.2159889
I	3906572.1583	9893456.7482739

In section A, the algorithms are tested and the optimization performance of IWOA is better than the other three algorithms in general, and WOA is slightly better than PSO and GWO; therefore, in this section, only two algorithms, IWOA and WOA, are used for the simulation and comparison of the frequency tracking control PI Parameters optimization, in order to validate the PI Parameters optimization ability of IWOA.

According to the principle shown in Fig. 20 to use IWOA and WOA to optimize the frequency tracking control PI Parameters, the obtained PI Parameters are shown in Table 8.

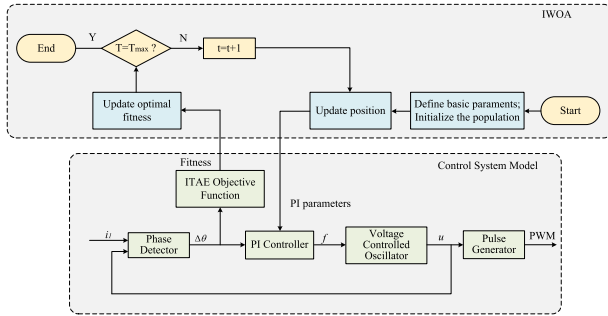


FIGURE 20. Schematic diagram of IWOA-PI parameters adjustment.

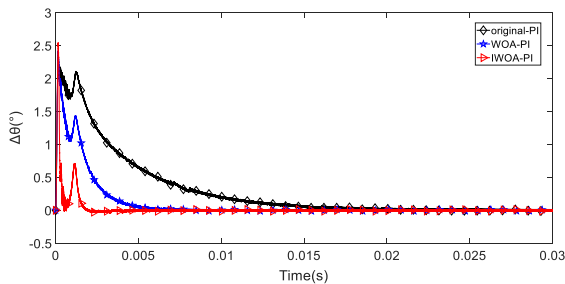


FIGURE 21. Phase difference curves between voltage and current at the transmitter of different PI Parameters.

The original PI Parameters obtained by the trial-and-error method and the optimized PI Parameters of WOA and IWOA are substituted into the MCR-WPT frequency tracking control system for Simulink simulation, respectively. The phase difference curves of the voltage and current at the transmitter for different PI Parameters are shown in Fig. 21.

It can be found that although the curve of IWOA-PI control has the largest phase difference at the very beginning, which reaches 2.5°, the difference with the curves of WOA-PI and original-PI control is not big, and the curve of IWOA-PI control quickly reduces to 0° within 0.005s, which is the fastest; the curve of WOA-PI control reduces the phase difference to 0° after 0.005s, which is medium speed; and the curve of original-PI control did not reduce the phase difference to 0° until 0.02s, which is the slowest.

It can be seen that the control performance of the PI Parameters derived from the IWOA optimization proposed in this paper is better, with fast response speed and high accuracy, and the IWOA is able to complete the optimization for the frequency tracking control PI Parameters better.

Since the policy complexity of IWOA is higher than that of WOA, the time spent in the optimization process of IWOA is inevitably longer, but this extra time loss is within the acceptable range. Moreover, in terms of control performance, the response time of IWOA-PI is about 40% of that of WOA-PI, indicating that the control effect of IWOA-PI is faster and better than that of WOA-PI. When the system is stabilized, the phase difference controlled by IWOA-PI is also kept at 0 degree at all times, indicating that the WPT system has been working in a resonant state. For manual parameterization,

it not only requires personnel to have rich experience and consumes time and energy, but also the parameters debugged may not be guaranteed to be optimal. Using IWOA, we can easily obtain the PI parameters with excellent results, which can help us find the optimal solution in a shorter time, thus reducing the investment of human resources.

V. CONCLUSION

MCR-WPT needs to use frequency tracking control method to keep the system in resonance state due to the characteristics of its own principle. And the parameters of the controller determine the control performance of the system. In order to save personnel’s energy and time for controller design and parameter tuning, this paper proposes to use an improved whale optimization algorithm to complete the PI parameter tuning of the frequency tracking controller. Regarding the improvement point part of the algorithm: firstly, the initialization of Kent chaotic mapping is used to improve the diversity of the initial solutions and accelerate the convergence speed of the algorithm; secondly, the balance between the global search and local search ability of the algorithm is considered, and adaptive weight coefficients are introduced to nonlinearly improve the convergence factor; finally, sine-cosine algorithmic strategy and Cauchy reverse learning strategy are introduced to avoid the problem that the algorithm is prone to precocious maturity. With the fusion of the above improvement points, IWOA outperforms other algorithms in eight benchmark function tests as well as the Wilcoxon rank sum test method, proving the superiority of the improved algorithm. Subsequently, IWOA and WOA are applied to the PI parameter optimization of frequency tracking control, and the phase difference curves under the control of different PI parameters are compared by simulation, in which the phase difference curve controlled by IWOA-PI parameters has the best effect and the fastest response speed. This shows that the improved algorithm proposed in this paper has a better performance for PI parameter tuning for frequency tracking control in wireless power transfer systems.

The improved algorithm proposed in this paper performs well in simulation applications, but the algorithm still has some limitations. Due to the integration of a variety of improvement strategies, the complexity of the algorithm increases, leading to an increase in computational cost, which will lead to an extension of the algorithm’s running time. For the benchmark function test as well as this paper’s frequency tracking control PI parameter tuning, although it is inevitable to increase some time overhead, but they are within the acceptable range. However, if facing other more complex problems, the improved algorithm in this paper needs to consume a lot of computation time, which may not be of great help to improve efficiency, and may also put the cart before the horse. In addition, the objective function established in this paper during the algorithm optimization process is the ITAE performance index. While ITAE is a useful optimization objective, it is only one of multiple considerations. PI gain does have a direct impact on the error index,

but it does not always directly reflect control effectiveness. Control effectiveness is a broader metric that includes system stability, response speed, overshoot, and regulation time. Moreover, it is essential to consider introducing a penalty to the control effort in the objective function, as this helps to improve the overall performance and stability of the system and allows us to better weigh the error against the use of the controller to find a better balance. Therefore, in future research, a more in-depth analysis of the system control factors is needed to obtain the control parameters with the best control effect by establishing a detailed and reasonable objective function.

REFERENCES

- [1] H. Xueliang, W. Wei, and T. Linlin, "Technical progress and application development of magnetic coupling resonant wireless power transfer," *Autom. Electric Power Syst.*, vol. 41, no. 2, p. 14, Jan. 2017.
- [2] S. Yunquan, L. Yangrui, and G. Jiating, "Research on wireless power transmission resistance matching based on LCC-S compensation structure," *Chin. J. Electron Devices*, vol. 43, no. 1, p. 6, 2020.
- [3] Q. Zhaopeng, W. Zhangyun, L. Hui, and C. Xiaorong, "Variable voltage wireless charging system for electric automobile based on series resonance compensation," *Chin. J. Electron Devices*, vol. 41, no. 3, p. 5, 2018.
- [4] L. Guojin, L. Yixin, C. Yulong, H. Kai, and B. Xinlei, "Frequency tracking control of wireless power transfer via magnetic resonance coupling based on FPGA," *Trans. China Electrotech. Soc.*, vol. 33, no. 14, pp. 3185–3193, 2018.
- [5] D. Wen, Y. Zou, Z. Li, and J. Yi, "Mixed-modulation method for adjusting frequency and voltage in the WPT systems with misalignments and load variations," *Prog. Electromagn. Res. B*, vol. 93, pp. 111–129, 2021.
- [6] Z. Zheng, N. Wang, and S. Ahmed, "Adaptive frequency tracking control with fuzzy PI compound controller for magnetically coupled resonant wireless power transfer," *Int. J. Fuzzy Syst.*, vol. 23, no. 6, pp. 1890–1903, Sep. 2021.
- [7] L. Yuanyuan, F. Hongwei, and F. Xi, "Adaptive fuzzy control of frequency tracking used in magnetic coupled resonance wireless power transfer system," *Chin. J. Electron Devices*, vol. 44, no. 6, pp. 1385–1391, 2021.
- [8] S. Ekinci and D. Izci, "Enhanced reptile search algorithm with Lévy flight for vehicle cruise control system design," *Evol. Intell.*, vol. 16, no. 4, pp. 1339–1351, Aug. 2023.
- [9] D. Izci, S. Ekinci, M. Kayri, and E. Eker, "A novel improved arithmetic optimization algorithm for optimal design of PID controlled and Bode's ideal transfer function based automobile cruise control system," *Evolving Syst.*, vol. 13, no. 3, pp. 453–468, Jun. 2022.
- [10] R. El-Khazali, "Fractional-order $PI\lambda D\mu$ controller design," *Comput. Math. Appl.*, vol. 66, no. 5, pp. 639–646, 2013.
- [11] D. Izci, S. Ekinci, H. L. Zeynelgil, and J. Hedley, "Performance evaluation of a novel improved slime mould algorithm for direct current motor and automatic voltage regulator systems," *Trans. Inst. Meas. Control*, vol. 44, no. 2, pp. 435–456, Jan. 2022.
- [12] F. D. J. Sorcia-Vázquez, J. Y. Rumbo-Morales, J. A. Brizuela-Mendoza, G. Ortiz-Torres, E. Sarmiento-Bustos, A. F. Pérez-Vidal, E. M. Rentería-Vargas, M. De-la-Torre, and R. Osorio-Sánchez, "Experimental validation of fractional PID controllers applied to a two-tank system," *Mathematics*, vol. 11, no. 12, p. 2651, Jun. 2023.
- [13] S. M. Ghamari, H. G. Narm, and H. Mollae, "Fractional-order fuzzy PID controller design on buck converter with antlion optimization algorithm," *IET Control Theory Appl.*, vol. 16, no. 3, pp. 340–352, 2022.
- [14] S. Mirjalili and A. Lewis, "The whale optimization algorithm," *Adv. Eng. Softw.*, vol. 95, pp. 51–67, May 2019, doi: 10.1016/j.advengsoft.2016.01.008.
- [15] K.-W. Huang, Z.-X. Wu, C.-L. Jiang, Z.-H. Huang, and S.-H. Lee, "WPO: A whale particle optimization algorithm," *Int. J. Comput. Intell. Syst.*, vol. 16, no. 1, p. 115, Jul. 2023.
- [16] Z. Shan, Y. Wang, X. Liu, and C. Wei, "Fuzzy automatic disturbance rejection control of quadrotor UAV based on improved whale optimization algorithm," *IEEE Access*, vol. 11, pp. 69117–69130, 2023.
- [17] J. Du, J. Hou, H. Wang, and Z. Chen, "Application of an improved whale optimization algorithm in time-optimal trajectory planning for manipulators," *Math. Biosci. Eng.*, vol. 20, no. 9, pp. 16304–16329, 2023.
- [18] W. Huang, J. Li, and D. Liu, "Real-time solution of unsteady inverse heat conduction problem based on parameter-adaptive PID with improved whale optimization algorithm," *Energies*, vol. 16, no. 1, p. 225, Dec. 2022.
- [19] X. S. Xiaoming Shi, K. L. Xiaoming Shi, and L. J. Kun Li, "Improved whale optimization algorithm via the inertia weight method based on the cosine function," *J. Internet Technol.*, vol. 23, no. 7, pp. 1623–1632, Dec. 2022.
- [20] W. Zichen, D. Zhenhai, D. Jun, S. Shuqian, and W. Chen, "Adaptive dynamic whale optimization algorithm based on multi-strategy improvement," *Comput. Eng. Design*, vol. 43, no. 9, p. 8, 2022.
- [21] G. Sun, Y. Shang, K. Yuan, and H. Gao, "An improved whale optimization algorithm based on nonlinear parameters and feedback mechanism," *Int. J. Comput. Intell. Syst.*, vol. 15, no. 1, p. 38, Dec. 2022.
- [22] R.-B. Wang, W.-F. Wang, L. Xu, J.-S. Pan, and S.-C. Chu, "Improved DV-Hop based on parallel and compact whale optimization algorithm for localization in wireless sensor networks," *Wireless Netw.*, vol. 28, no. 8, pp. 3411–3428, Nov. 2022.
- [23] X. Li, Q. Yang, H. Wu, S. Tan, Q. He, N. Wang, and X. Yang, "Joints trajectory planning of robot based on slime mould whale optimization algorithm," *Algorithms*, vol. 15, no. 10, p. 363, Sep. 2022.
- [24] Y. Liu, F. Liu, H. Feng, G. Zhang, L. Wang, R. Chi, and K. Li, "Frequency tracking control of the WPT system based on fuzzy RBF neural network," *Int. J. Intell. Syst.*, vol. 37, no. 7, pp. 3881–3899, Jul. 2022.
- [25] L. Jianjun, S. Dingyuan, and W. Guoning, "Hybrid chaotic optimization algorithm based on Kent map," *Comput. Eng. Design*, vol. 36, no. 6, pp. 1498–1503, 2015.



XIONG YANG received the Ph.D. degree from Hohai University, in 2015. He is currently a Senior Engineer with the Department of Distribution Network Technology, State Grid Jiangsu Electric Power Company Ltd., Research Institute. His research interests include distribution automation, grid connection of distributed new energy, and energy storage technology.



JIAMIN GUAN received the bachelor's degree from the Nanjing Institute of Technology, Nanjing, China, in 2021, where he is currently pursuing the master's degree. His research interests include wireless power transfer systems, advanced control technology, and optimization algorithms.

...